Arsenic(V) Immobilization in Fly Ash and Lead-Zinc Mine Tailing-based Geopolymer: Performance and Mechanism Insight

Alseny Bah, Jie Jin, Andrea O. Ramos, Feihu Li*

Abstract: Global mining activities produce thousands of millions of toxic-bearing mine tailing (MT) wastes each year. Storage of the mine tailings not only encroaches upon large areas of cropland but also arouses additional ecological and environmental risks especially when the toxics (e.g., arsenic) are leached out during the stormy weather. Herein we demonstrate that geopolymerization of a mixture of the toxic-bearing mine tailings and the coal fly ash (FA) with a blending of sodium hydroxide (NaOH) and sodium silicate solution can effectively immobilize extra arsenic (As) species derived from arsenic-bearing wastes in the geopolymer specimens, which also possess high compressive strengths (e.g., > 25 MPa for specimens with 54 wt.% FA and activated with 10 M NaOH), allowing them to be further used as low-carbon, cement-free building materials. The geopolymer strength was found to depend clearly upon the NaOH concentration, the fly ash content, the arsenic content, and the curing time, with the maximum being 37.07 MPa for a specimen with 54 wt.% FA, 0.03 wt.% As activated with 10 M NaOH and cured for 28 days. Leaching tests showed that all specimens can achieve an immobilization efficiency as high as 95.4% toward As, and that the leachabilities of both As and other toxic heavy metals are far below the limits of the Chinese leaching standard for hazardous wastes (GB 5085.3 − 2007). Microstructural analyses using X-ray diffractometer (XRD), scanning electron microscopic (SEM), Fourier transform infrared (FTIR) indicate that the As species was physically encapsulated along with the formation of geopolymer gels at first, and then chemically incorporated into the crystalline phases (e.g., calcium silicate, and calcium silicate hydroxide) derived from the geopolymer gels as a result of prolonging the curing time. The developed FA/MT-based geopolymers represent a promising green material for both the remediation of As-bearing lands and the construction industry.

INTRODUCTION

Arsenic (As) contamination in water environments (e.g., mine drainage, groundwater, etc.) and soils due to mining activities have raised the risk of arsenic exposure to crop plants (e.g., rice), animals, and humans, and thus aroused growing concern from across the world.[1] China holds approximately 70% of the world's arsenic reservoirs.[2] The mining of lead, zinc, and copper ores produced over 32 million tons of arsenic-bearing mine tailing (MT) wastes annually, predominantly in Hunan province, China.[3] In severe situations, these arsenic residues can contaminate the surrounding soils and groundwater, causing serious threats to the sustainability of agroecosystems and food safety. To address this issue, a variety of technologies, including adsorption, bioremediation, chemical-enhanced washing, chemical precipitation, electro-coagulation, electrokinetic method, ion-exchange, membrane filtration, phytoremediation, solidification/stabilization (S/S), etc. have been widely exploited and well documented in the literature.[4-8] In terms of soil remediation, adsorption, chemical-enhanced washing, chemical precipitation, and phytoremediation are effective in sequestering and/or immobilizing arsenic, however, both the economic and the environmental restrictions limit their application on a large scale.[9]

Pozzolanic-based solidification/stabilization (S/S) is a well-established, effective, yet cost-efficient remediation technology to immobilize hazardous wastes in contaminated soils and sludges.[10] Arsenic can be effectively immobilized using ordinary Portland cement (OPC)[11-14] and magnesium phosphate cement[15-16] as the major cementitious materials. However, the high carbon footprint associated with the production of both types of cement makes the cement-based S/S technology less appealing in the scenario of global carbon neutrality by the middle of the century.[17] To this end, low-carbon, high-efficiency S/S technologies using massive industrial by-products, e.g., fly ash, red mud, blast-furnace and/or smelting slag, mine tailing, flue gas desulfurization (FGD) gypsum, etc. as the alternative cementitious materials have received much attention and been extensively studied.[2, 15, 18-20]

Of various S/S technologies, geopolymerization of the mixture of arsenic-bearing waste and the silica- and/or alumina-rich industrial solid wastes (e.g., fly ash, red mud, mine tailing, etc.) by alkali activation has been demonstrated to be an effective alternative to immobilize arsenic into the geopolymer matrix.[18-19, 21-23] Geopolymer binders derived from both the alkali activation of coal fly ash[21] and the high-energy ball milling activation of granulated lead smelting slag[22] have shown excellent ability to stabilize the municipal solid waste incinerator fly ash (MSWI FA) with high arsenic content. Recently, it was reported that red mud-metakaolin (MK) based geopolymer shows a good arsenic retention capability as well as a high compressive strength (~ 15 MPa), making it an environmentally friendly backfilling material for sustainable remediation of arsenic pollution.[19] However, the production of MK by calcining kaolinite (at 700 °C) can yield high CO_2 emissions, even though kaolinite clays (> 40% kaolinite) are inexpensive and widely accessible.[24] Compared to metakaolin-based geopolymers, mine tailing-based geopolymers have a lower carbon footprint, making them more desirable for use as building materials and as a matrix for immobilizing toxic wastes.[23, 25-27] For instance, when using sugar mill lime sludge as a Ca-based activator, it was suggested that coal fly ash and mine tailing-based geopolymer can effectively stabilize the mine tailings with high levels of arsenic and heavy metals. Besides, since the geopolymer has high compressive strength (> 7.5 MPa), it can also be used as construction materials.[23]

While many studies have demonstrated that geopolymer matrix plays a crucial role in the immobilization of arsenic wastes, the underlying mechanisms remain poorly understood due to the contradictory results that have often been presented. During the geopolymerization process, arsenic can react either with calcium-rich components to form calcium arsenate precipitates, with Friedel's salt to yield As-Friedel's salt mineral, or with the geopolymer gels (e.g., calcium silicate hydrate (CSH), calcium aluminum hydrate (CAH)) to form surface complexes.[20, 22] Zhou *et al.* claimed that ion exchange with ettringite, formation of Ca-As and Fe-As precipitates, and physical encapsulation with geopolymer gel were the predominant mechanisms for stabilizing arsenic.[19] However, other studies showed that arsenic exhibits a poor immobilization potential in geopolymer systems due to its high pH sensitivity.[28-29] In this regard, the interactions between

Table 1 | Geopolymer specimen composition matrix and characterization tests conducted.

Specimen ID	NaOH (M)	FA content (wt.%)	GY content (wt.%)	As^V content (wt.%)	Si/Al [a]	Na/Al [a]	Curing time (days)	UCS test	XRD	SEM	FTIR
FMA5G-02a	5	54	2.5	0.01	0.83	0.41	7, 14, 28	X		X	
FMA5G-02b	5	54	2.5	0.03	0.83	0.41	7, 14, 28	X	X	X	X
FMA5G-02c	5	54	2.5	0.05	0.83	0.41	7, 14, 28	X		X	
FMA8G-02a	8	54	2.5	0.01	0.83	0.52	7, 14, 28	X			
FMA8G-02b	8	54	2.5	0.03	0.83	0.52	7, 14, 28	X		X	
FMA8G-02c	8	54	2.5	0.05	0.83	0.52	7, 14, 28	X	X	X	X
FMA10G-01a	10	61	2.5	0.01	0.94	0.46	7, 14, 28	X	X	X	
FMA10G-01b	10	61	2.5	0.03	0.94	0.46	7, 14, 28	X			
FMA10G-01c	10	61	2.5	0.05	0.94	0.46	7, 14, 28	X		X	
FMA10G-02a	10	54	2.5	0.01	0.83	0.60	7, 14, 28	X	X	X	X
FMA10G-02b	10	54	2.5	0.03	0.83	0.60	7, 14, 28	X	X	X	X
FMA10G-02c	10	54	2.5	0.05	0.83	0.60	7, 14, 28	X	X	X	X
FMA10G-03a	10	44	2.5	0.01	0.68	0.87	7, 14, 28	X		X	
FMA10G-03b	10	44	2.5	0.03	0.68	0.87	7, 14, 28	X			
FMA10G-03c	10	44	2.5	0.05	0.68	0.87	7, 14, 28	X		X	
FMA10G-04a	10	28	2.5	0.01	0.43	1.62	7, 14, 28	X		X	
FMA10G-04b	10	28	2.5	0.03	0.43	1.62	7, 14, 28	X			
FMA10G-04c	10	28	2.5	0.05	0.43	1.62	7, 14, 28	X			
FMA5G5-02a	5	54	5	0.01	0.83	0.41	7, 14, 28	X			
FMA5G5-02b	5	54	5	0.03	0.83	0.41	7, 14, 28	X			
FMA5G5-02c	5	54	5	0.05	0.83	0.41	7, 14, 28	X			
FMA8G5-02a	8	54	5	0.01	0.83	0.52	7, 14, 28	X	X	X	X
FMA8G5-02b	8	54	5	0.03	0.83	0.52	7, 14, 28	X		X	
FMA8G5-02c	8	54	5	0.05	0.83	0.52	7, 14, 28	X			
FMA10G5-02a	10	54	5	0.01	0.83	0.60	7, 14, 28	X	X	X	X
FMA10G5-02b	10	54	5	0.03	0.83	0.60	7, 14, 28	X			
FMA10G5-02c	10	54	5	0.05	0.83	0.60	7, 14, 28	X		X	

[a] Note: the calculated Si/Al and Na/Al ratios in the initial mixtures are not necessarily the same as the final ratios in the geopolymer gels.

arsenic and the mine tailing-based geopolymer matrix and the immobilization mechanism of arsenic should be further elucidated.

In this study, we focus on the feasibility of immobilizing arsenate (As^V) in geopolymer matrices derived from the mixtures of fly ash, lead-zinc mine tailing, and FGD gypsum that were activated with sodium hydroxide and sodium silicate solution. The geopolymer specimens were investigated at different As^V contents, NaOH concentrations, FA contents, GY contents, curing time, etc. to explore the mechanic properties, microstructure, As^V leaching characteristics, and the immobilization mechanism of arsenic by using unconfined compressive strength (UCS) test, X-ray diffraction (XRD), scanning electron microscopy (SEM), and Fourier Transform Infrared (FTIR) analyses.

MATERIALS AND METHODS

Materials. The raw materials used in this study include lead-zinc (Pb-Zn) mine tailings (MT), class F fly ash (FA), and FGD gypsum (GY). Both the FA and the GY were obtained from Jiangsu Nanre Power Generation Co., Ltd. (Nanjing, China). The MT was provided by Nanjing Yinmao Pb-Zn Mining Industry Co., Ltd. (Nanjing, China). The physicochemical characteristics of both the FA and the MT can be found elsewhere.[27] The GY consists of kidney bean-shaped gypsum ($CaSO_4{\cdot}2H_2O$, JCPDS #33-0311) powders of size ranging from ~ 10 to ~ 55 μm (see Figure S1 in the Supporting Information).

Reagent grade 96% NaOH pellets were purchased from Macklin Biochemical Co., Ltd. (Shanghai, China). Sodium silicate (SS) solution with silica to sodium oxide molar ratio of 2:2 − 2.31 was obtained from Ganjiashan Yourui Refractories Co., Ltd. (Nanjing, China). Sodium arsenate dibasic heptahydrate ($Na_2HAsO_4{\cdot}7H_2O$, 98%) was purchased from Sigma-Aldrich (Shanghai, China) and used as the arsenate source. All the chemicals were used as received without further purification. Deionized water was used in preparation solutions and the geopolymer.

Preparation and characterization of geopolymer. For the preparation of FA/MT-based geopolymer, FA was fully mixed with MT at a given content, i.e., 28, 44, 54, and 61 wt.% (by total solid mass) to form a dry-blend. Then the NaOH (5, 8, and 10 M) together with 25 g of SS and deionized water were slowly added to the above dry-blend while mixing gently until a homogeneous paste was formed. The liquid to solid (L/S) ratio was kept at 0.3 – 0.4 to achieve a paste with good workability. The resultant paste was then cast into the six-in-one cubic steel molds (20 × 20 × 20 mm^3) at room temperature for 24 h. The shaped cubic geopolymer specimens were demolded carefully and placed in an oven for curing at 65 °C for another 24 h. After cooling, the specimens were left in the lab tray and cured at room temperature for 7, 14, and 28 days before further tests. All the geopolymer specimens were prepared in triplicate. To study the effect of GY content on the mechanical strength as well as the As^V immobilization performance of the FA/MT-based geopolymer specimens, 2.5 and 5 wt.% of GY (by total solid mass) were added into the dry-blend. In the case of preparing geopolymer for As^V immobilization, 0.01, 0.03, and 0.05 wt.% of arsenic were added along with the NaOH solution. The geopolymer specimen composition matrix is summarized in Table 1.

The unconfined compressive strength (UCS) tests were performed to evaluate the effects of NaOH concentration, incorporated GY, curing time, and introduction of As^V on the mechanical strength of the resultant geopolymer specimens. After 7-, 14-, and 28-day curing, the geopolymer specimens were tested

on a WDW-100 universal material testing machine (Jinan Fangyuan Test Instrument Co., Ltd., China) at a constant loading of 5 MPa/s in terms of the ASTM C109M-2008 standard. Each geopolymer sample was tested in triplicate and the average UCS value was used for further analysis.

To investigate the microscopic characteristics of geopolymer, the crushed specimens from the UCS tests were collected and further milled into fine powders for further tests. X-ray diffraction (XRD) analysis was conducted on an XRD-6100 diffractometer (Shimadzu, Japan) at a tube voltage of 40 kV and a tube current of 30 mA with Cu-Kα radiation (step size: 0.02, scanning rate: 5°/min). The morphological images of the geopolymer specimens were obtained on a SU1510 (Hitachi, Japan) scanning electron microscope (SEM) at an accelerating voltage of 1.5 kV. Fourier Transform Infrared Spectroscopy (FTIR) data were collected on Is5 infrared spectrometer (Thermo Nicolet, USA) by using the KBr pellet method.

Leaching tests. To evaluate the As^V immobilization performance of the FA/MT-geopolymers, the Toxicity Characteristic Leaching Procedure (TCLP) procedure tests were conducted following the US EPA test method 1311.[30] The leachates were filtered with 0.45 μm filters (Tianjin Navigator Lab Instrument Co., Ltd, China) and acidified with ultrapure nitric acid (Sinopharm Chemical, Shanghai, China) before further analyses. As^V concentrations in the leachates were measured using an Optima 8000 Inductively Coupled Plasma-Optical Emission Spectrometry (ICP-OES) analyzer (PerkinElmer Inc., USA). All the TCLP tests were performed in triplicate and average values were used. The As^V immobilization efficiency was determined using the following equation,

$$Immobilization\% = \frac{C_0 - C_f}{C_0} \times 100\%$$

where $\mathbf{C}_0$ is the As^V concentration in the initial suspension of the TCLP test by assuming that all As^V in the geopolymer specimens are leachable, while $\mathbf{C}_f$ is the measured As^V concentration in the corresponding leachate ($mg \cdot L^{-1}$).

RESULTS AND DISCUSSIONS

Effect of NaOH concentration on UCS of the FA/MT-based geopolymers. To investigate the effect of NaOH concentration on the UCS of the FA/MT-based geopolymers, UCS tests were performed on geopolymer specimens with different FA and As^V contents that were activated with 5, 8, and 10 M NaOH, respectively (Figures 1a, 1b, S2 and S3). As in the case in Figure 1a, apart from geopolymers with 28 wt.% of FA, the UCS values after curing for 7 days (abbreviated as 7-day UCS) of the FA/MT-based geopolymers increase almost linearly with increasing NaOH concentrations ranging from 5 to 10 M. This near-linear dependency between the UCS and the NaOH concentration is also evident for these geopolymer specimens cured for 14, and 28 days, respectively (Figures S2 and S3). It is well established that NaOH accelerates the dissolution of silicates and aluminosilicates in aqueous systems.[31] With increasing NaOH concentrations, UCS is likely to increase because more Na^+ and OH^- react with the silica- and alumina-rich phase, dissolving more Si and Al and thereby increasing the concentration of Si and Al in the liquid phase.[32] Faster dissolution of the aluminosilicate phases may lead to faster geopolymer formation due to rapid conversion of the raw materials. Besides, it is believed that during the formation of geopolymer, Na^+ and OH^- ions also play significant roles in stabilizing aqueous species and colloids, increasing the solubility limits of silica and alumina, reducing electrostatic repulsion between the dissolved anions, and catalyzing geopolymer gel formation and rearrangement.[31] These will in turn lead to faster geopolymer formation, and thereby increase the geopolymer compressive strength. The UCS improvement with NaOH concentration has also been observed previously,[27, 31-34] especially in mixtures with a large number of amorphous aluminosilicate phases.[32, 35] This observation is also validated in the present study that the activation of the FA/MT mixtures with 10 M NaOH resulted in the highest UCS (i.e., 35.52 and 37.07 MPa for 7-day and 28-day UCS, respectively) when the mixture with FA content as high as 54 wt.% was used (Figures 1a and S2b). This is because FA particles contain more amorphous phases than the MT powder and are thereby more reactive to the NaOH solution.[27]

It is of interest to note, however, that the UCS value of geopolymer specimen activated with 10 M NaOH is lower than that activated with 8 M NaOH in the case of geopolymers with 28 wt.% of FA (Figures 1a and S2). This can be explained by the negative effect of excess NaOH on geopolymer formation which has also been observed previously.[31, 36] Geopolymer compressive strength is believed to increase with increasing Na/Al molar ratios up to a specific maximum value, above which the strength is

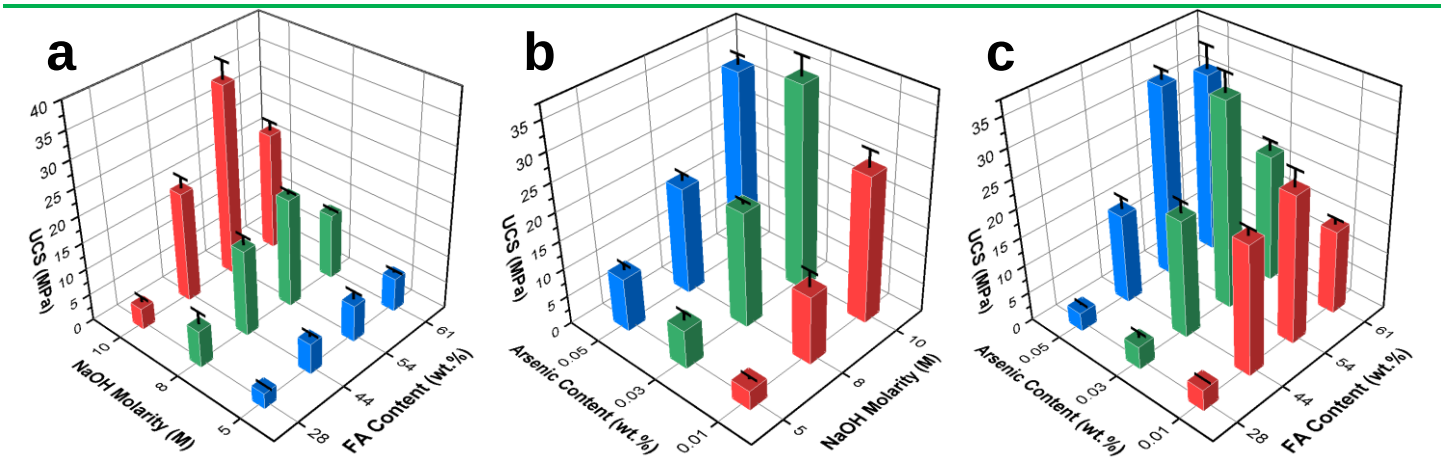

Figure 1 | (**a**) Effect of NaOH concentration and FA content on the 7-day UCS of FT/MT-based geopolymer specimens with a constant As^V content of 0.03 wt.%, (**b**) Effect of NaOH concentration and As^V content on the 7-day UCS of specimens with a constant FA content of 54 wt.%, (**c**) Effect of As^V and FA contents on the 7-day UCS of specimens activated with 10 M NaOH.

reduced. [31, 36] Based on this argument, it would appear that the Na/Al molar ratio has reached up to the maximum value favorable for the geopolymer formation in the specimen with 28 wt.% of FA that was activated with 8 M NaOH.

Effect of FA, AsV and GY contents on UCS. As shown in Figures 1a and S2, all the UCS values (i.e., 7-, 14- and 28-day UCS) increase with FA contents ranging from 28 to 54 wt.%, while decrease to some extent when the FA contents are as high as 61 wt.% at NaOH concentrations of 5, 8 and 10 M, respectively. As discussed above, it appears that the Na/Al molar ratios have achieved the optimum value favoring geopolymer formation when the FA contents increased up to 54 wt.%, indicating that the FA/MT mixture containing 54 wt.% FA is the optimal recipe for geopolymer formation regarding the compressive strength. Further increasing the FA proportion in the FA/MT mixtures will no doubt result in decreased Na/Al molar ratios, and thus declined compressive strengths. This behavior is in good consistency with the calculated Na/Al data (Table 1) and has also been reported elsewhere.[37]

In general, Na^+ ions from the alkali activator (e.g., NaOH) can reduce the electrostatic repulsion between the dissolved anions through the formation of ion-pairing complexes (e.g., $Si/Al–O^- \cdots Na^+$), by which to accelerate the geopolymer gel formation.[31] As mentioned above, 0.01 – 0.05 wt.% of As^V was added to the geopolymer mixtures in the form of sodium arsenate to evaluate the immobilization performance in this study. This suggests that the Na^+ ions from sodium arsenate will somewhat contribute to the geopolymer gel formation, especially when the Na^+ ions from NaOH are very limited. The effect of As^V content on the UCS is distinct in the cases of geopolymer specimens with 54 wt.% of FA and 5 M NaOH, which demonstrates that the UCS values increase proportionally as the As^V contents increase from 0.01 wt.% to 0.05 wt.% (Figures 1b and S3), confirming the profound contribution from the Na^+ ions of sodium arsenate. Similar observations are also notable in geopolymer specimens with 61 wt.% FA and 10 M NaOH as shown in Figures 1c and S4, where Na^+ ions from NaOH are inadequate to dissolve the amorphous phases in FA of the mixtures, and therefore the introduction of extra Na^+ ions along

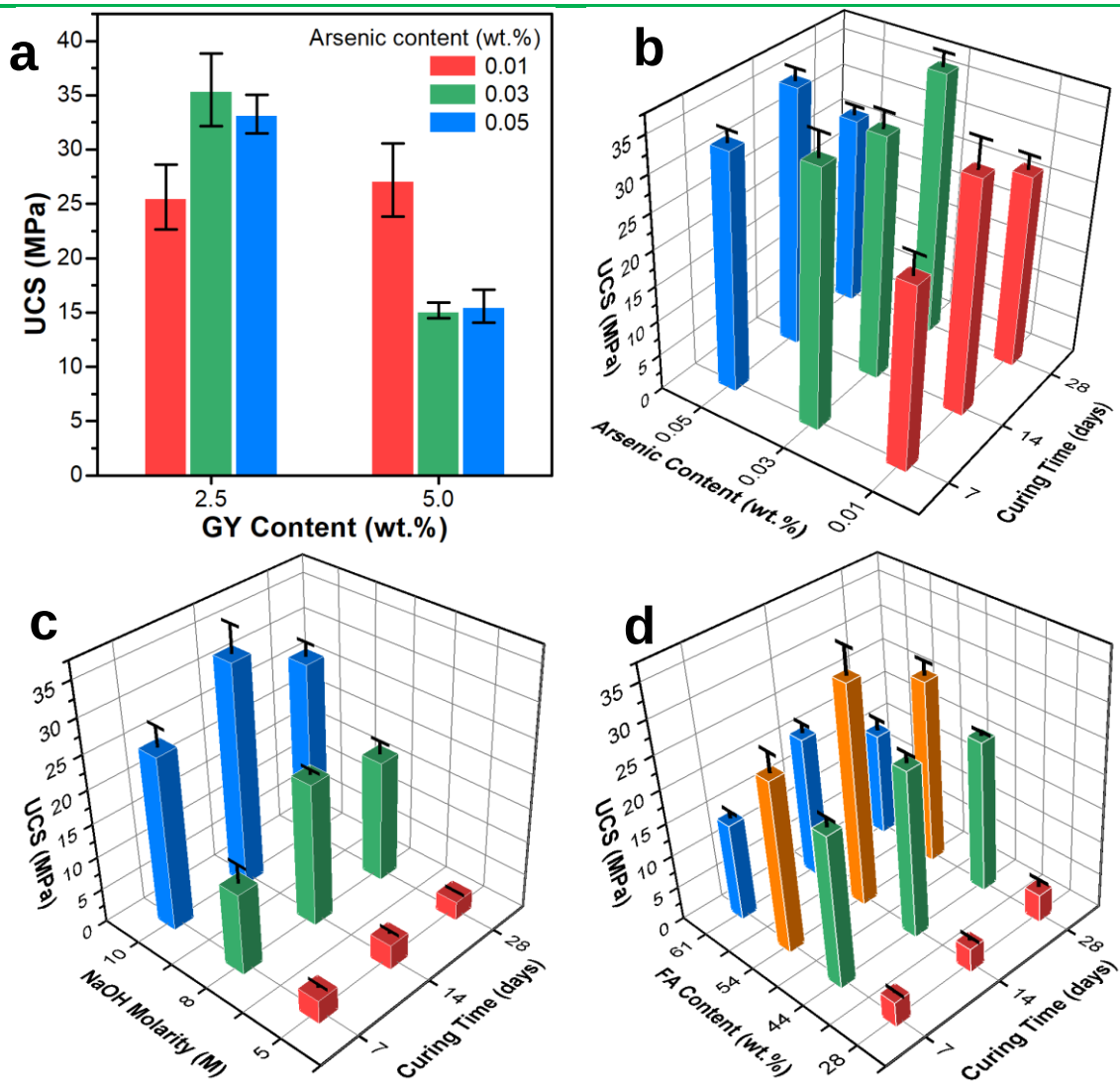

Figure 2 | (**a**) Effect of GY content on the 7-day UCS of specimens (54 wt.% FA, 10 M NaOH); (**b**) Effect of curing time and As^V content on the UCS of the same specimens; (**c**) Effect of curing time and NaOH concentration on the UCS of specimens (54 wt.% FA, and 0.01 wt.% As^V); and (**d**) Effect of curing time and FA content on the UCS of specimens (0.01 wt.% As^V, and 10 M NaOH).

with As^V sources can result in obvious increases in the compressive strengths. In other geopolymer specimens rich in Na^+ ions from NaOH (with high Na/Al molar ratios) as shown in Figures 1b, 1c, S3, and S4, the effect of As^V content appears to be stochastic since excess Na^+ ions in the geopolymer system can reduce the compressive strength.[31, 36]

Gypsum is known to accelerate the induration and the early strength of the geopolymer, promoting arsenic solidification to some extent.[2, 10, 38-39] Nevertheless, excess gypsum in geopolymer mixture appears to increase the mobility of arsenic,[2, 40] and reduce the compressive strength of the resultant geopolymer. For the leachability of toxics and the compressive strength, the addition of 8 – 12 wt.% of gypsum to the geopolymer mixture is well established in the literature.[2, 39] However, our results in Figure 2a demonstrate that introduction of 5 wt.% of FGD gypsum can lead to significant decreases in the UCS values of geopolymers (NaOH = 10 M, FA content = 54 wt.%), as compared to those with 2.5 wt.% gypsums. Therefore, we mainly focus on the geopolymer mixtures with a GY content of 2.5 wt.% in the present study, and all geopolymer mixtures were blended with 2.5 wt.% of GY unless otherwise specified. Moreover, it is worthy to note that the highest UCS of 39.46 MPa can be found in geopolymer specimens with 61 wt.% FA, 0.05 wt.% As^V and 10 M NaOH after curing for 14 days (see the supplementary UCS data). Besides, this geopolymer has a 28-day UCS as high as 31.88 MPa. In comparison to conventional FA-based geopolymers,[18, 20, 22, 32] the geopolymer exhibits superior compressive strength, making it an attractive material for use in construction.

Effect of curing time on UCS. It has been reported previously that for FA-based geopolymer systems the temperature at which specimens are cured significantly affects its final compressive strength.[41] Our previous work has also confirmed that curing at 65 °C can improve the overall strength of the geopolymer specimens as compared to those cured at 25 °C.[27] Therefore, the effect of curing time on UCS in this study was investigated by evaluating the compressive strength of specimens cured at 65 °C for different curing times. Geopolymer specimens prepared with varying FA and As^V contents, NaOH concentrations, and cured for 7, 14, and 28 days were evaluated and the results are presented in Figure 2b–d. For all specimens, it appears that the strength of the geopolymers developed rapidly in the first 7 days, accounting for > 70% of the maximum UCS values that were obtained in 14 days. This observation is in good agreement with previous reports.[27, 42-43]

However, it is of interest to note that the 28-day UCS values decreased slightly (i.e., 9.2 – 16.6%) as compared to the 14-day UCS for most specimens studied (Figure 2b–d). This may attribute to the structural weakening of geopolymer gels due to the loss of structural water during the curing at elevated temperature (i.e., 65 °C),[41] and the reduction in compactness owing to the phase transitions from amorphous gels to crystalline minerals.[16, 18] Nevertheless, it is apparent that when the specimen was prepared with 54 wt.% FA and 10 M NaOH, curing at 65 °C for 24 hours can endow the specimen with a 7-day UCS as high as 35.52 MPa (Figure 2b), implying that curing at elevated temperature can not only enhance the early strength of the specimen but also shorten the curing time.[44]

Leaching results of As^V. For geopolymer formation, a compacted and consolidated material with relatively high strength is usually preferable, while low permeability is desirable from a leaching point of view when using such geopolymer for the solidification/stabilization of toxic wastes. The TCLP leaching results of As^V from the geopolymer specimens with different compositions and curing times are given in Table 2 and depicted in Figure 3. The results are quite variable, with leached As^V concentrations in the leachates (i.e., the As^V leachabilities) ranging from 0 (not detected, n.d.) to 2.6 mg/L (Table 2). In the case of geopolymer specimens with 54 wt.% of FA and 10 M of NaOH, curing in the air for 7 days endowed the specimen of 0.03 wt.% As^V with the maximum strength (i.e., 35.52 MPa), while presented the highest As^V leachability (i.e., 2.16 mg/L) to the specimen with 0.05 wt.% As^V (Figure 3a). However, when prolonging the curing time to 14 days, it is of interest to note that both the UCS values and the As^V leachabilities increase proportionally with the As^V contents from 0.01 to 0.05 wt.%, which has also been observed previously.[45] Further extending the curing time to 28 days resulted in the maximum strength of the specimen with 0.03 wt.% As^V (i.e., 37.07 MPa), while the highest As^V leachability of that incorporating 0.05 wt.% of As^V (i.e., 1.4 mg/L). This observation indicates that it is difficult to correlate the As^V leachability, i.e., the immobilization performance for As^V, with the As^V content, the UCS, and the curing time. Besides immobilization by geopolymerization, As^V is also possible fixed by precipitate formation such as calcium arsenate hydrates.[12, 20]

Table 2 | As^V leaching test results of geopolymer specimens with different curing time.

Specimen ID	As^V leachability (mg/L)			Specimen ID	As^V leachability (mg/L)			Specimen ID	As^V leachability (mg/L)		
	7 days	14 days	28 days		7 days	14 days	28 days		7 days	14 days	28 days
FMA5G-02a	0.27	0.75	n.d.	FMA10G-02a	0.31	0.02	0.01	FMA5G5-02a	0.48	0.18	n.a.
FMA5G-02b	2.17	1.11	0.84	FMA10G-02b	1.33	0.61	0.01	FMA5G5-02b	0.94	1.42	1.00
FMA5G-02c	2.17	1.96	2.09	FMA10G-02c	2.16	1.87	1.37	FMA5G5-02c	n.d.	2.56	0.87
FMA8G-02a	0.34	1.32	n.d.	FMA10G-03a	0.12	n.d.	0.65	FMA8G5-02a	0.83	n.d.	n.d.
FMA8G-02b	0.58	0.72	0.22	FMA10G-03b	n. d.	0.95	0.09	FMA8G5-02b	1.05	1.33	n.d.
FMA8G-02c	0.82	n. d.	0.83	FMA10G-03c	2.53	1.87	0.78	FMA8G5-02c	2.60	n.d.	1.77
FMA10G-01a	0.08	0.44	0.06	FMA10G-04a	0.70	n. d.	0.41	FMA10G5-02a	0.08	1.05	n.a.
FMA10G-01b	0.57	0.63	0.31	FMA10G-04b	n. d.	0.59	0.07	FMA10G5-02b	1.05	0.81	0.13
FMA10G-01c	0.89	1.20	n.a.	FMA10G-04c	0.94	1.19	0.20	FMA10G5-02c	1.16	0.99	1.44
Chinese standard	**5.0**	**5.0**	**5.0**								

* n.d. = not detected; n.a. = not available.

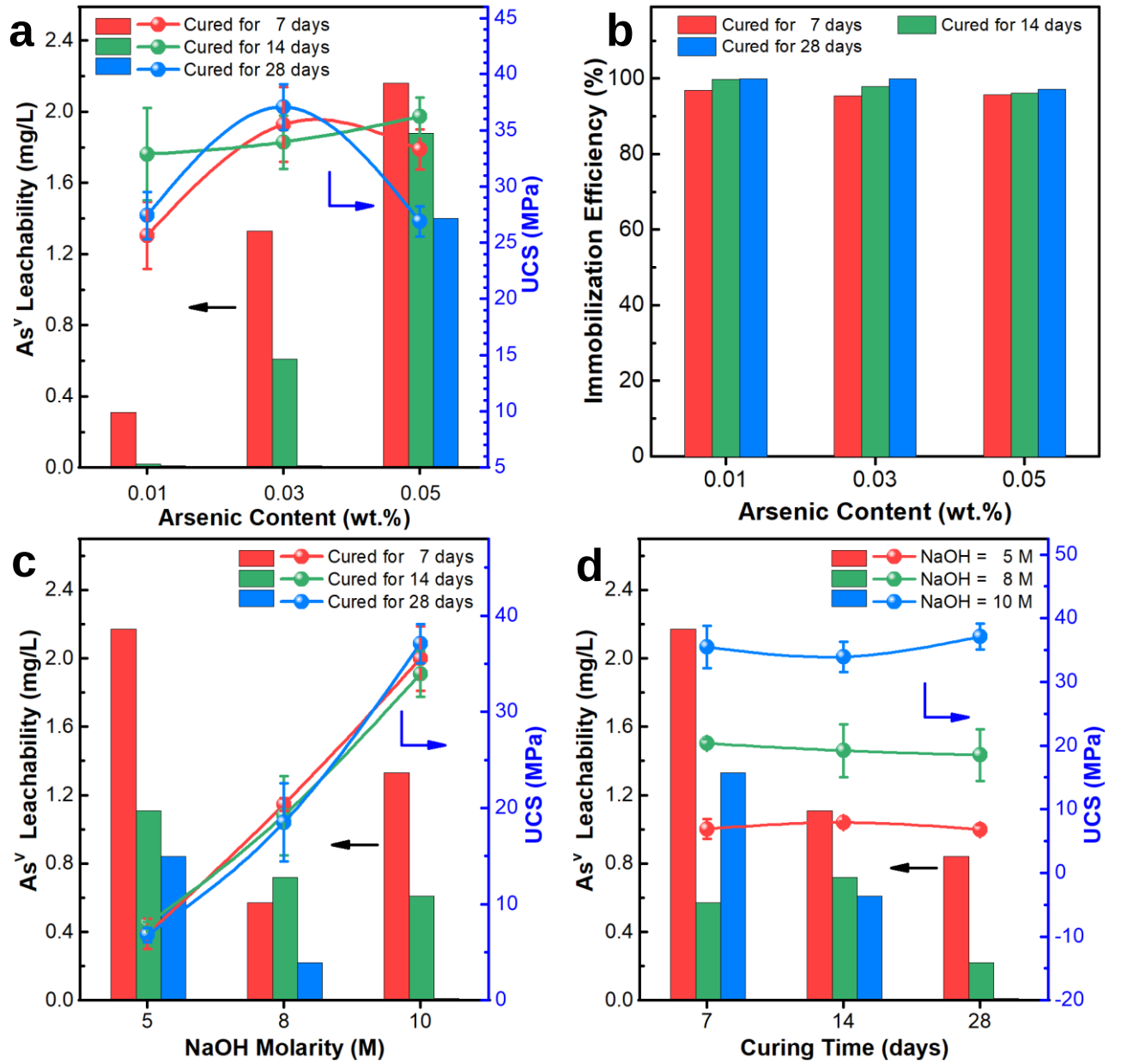

Figure 3 | Effect of As^V content on (**a**) the As^V leachability and the 7-day UCS, and (**b**) the As^V immobilization efficiency of geopolymer specimens (54 wt.% FA, 10 M NaOH), (**c**) Effect of NaOH concentration on the As^V leachability and the UCS of specimens cured for 7, 14, and 28 days (54 wt.% FA, and 0.03 wt.% As^V), (**d**) Effect of curing time on the As^V leachability and the UCS of specimens with 5, 8, and 10 M NaOH (54 wt.% FA, and 0.03 wt.% As^V).

Results in Figure 3c indicate that the As^V leachability decreases with increasing NaOH concentrations from 5 to 10 M for specimens with 54 wt.% of FA, 0.03 wt.% As^V and cured for 14, and 28 days, respectively, whereas the UCS values increase proportionally with the NaOH concentrations as discussed above. This can be explained by the fact that higher NaOH concentration can lead to the faster dissolution of the aluminosilicate phases, and thereby faster geopolymer formation,[31-32] by which free As^V were consolidated and in turn stabilized.[22-23] Furthermore, it is evident that extending the curing time from 7 to 28 days does not improve the compressive strength of these specimens too much (Figure 3d) since specimens are likely to reach their ultimate compressive strength in 7 days for FA/MT-based geopolymer.[42] However, prolonging the curing time can significantly reduce the As^V leachabilities. For instance, in specimen with 54 wt.% of FA, 0.03 wt.% of As^V and activated with 10 M NaOH (i.e., FMA10G-02b), a reduction of As^V leachability from 1.33 mg/L to 0.01 mg/L was observed when extending the curing time from 7 to 28 days (Table 2). This is in good agreement with the previous report,[46] confirming that increased curing time appears to reduce the water permeability and porosity of the geopolymer, and thereby enhance the As^V S/S performance as expected.

Besides, the As^V immobilization efficiencies of all geopolymer specimens are above 95.4% (Figure 3b), and As^V leachabilities of all specimens are below 5.0 mg/L as specified in the standard (Table 2). Moreover, the leachabilities of other heavy metal ions

including copper (Cu), cadmium (Cd), lead (Pb), and chromium (Cr) are also below the maximum toxic levels (Table S1), indicating that all specimens comply with the Chinese leaching standard for hazardous wastes (GB 5085.3 − 2007).[47] Therefore, the FA/MT-based geopolymers demonstrated superior immobilization performance for both As^V and typical heavy metals and high compressive strengths, especially in specimens with 54 wt.% of FA activated with 10 M NaOH (i.e., the FMA10G-02 series). Given the performance of mechanical strengths and contaminant immobilization, FA/MT-based geopolymers can be used for the synchronous S/S of As^V and heavy metal-contaminated soil and sediments.

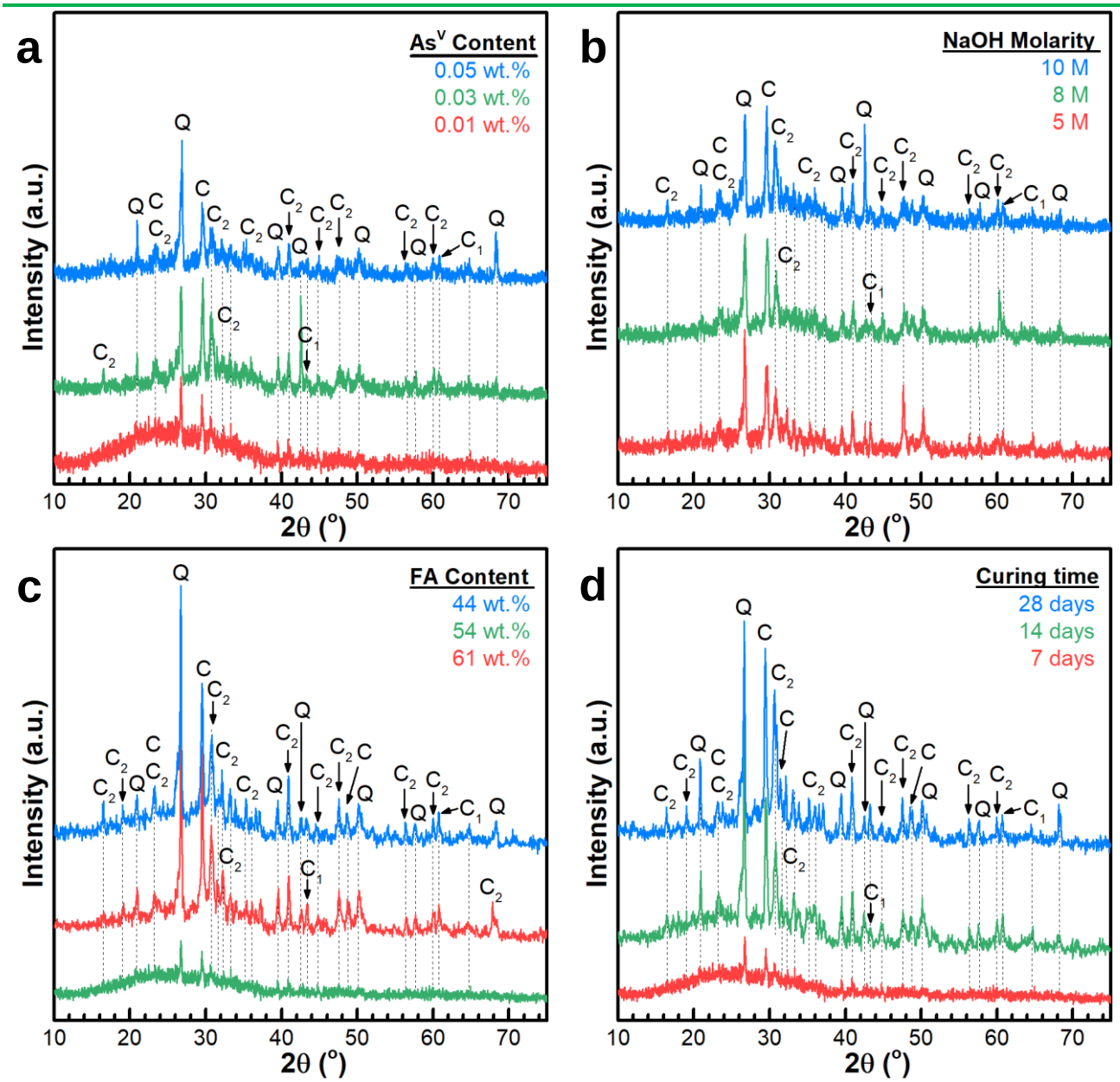

Figure 4 | XRD patterns of (**a**) geopolymer specimens of 54 wt.% FA, 10 M NaOH and cured for 7 days with varying arsenic contents; (**b**) specimens of 54 wt.% FA, 0.03 wt.% As^V, cured for 7 days and activated with 5, 8, and 10 M NaOH; (**c**) specimens of 0.01 wt.% As^V, 10 M NaOH and cured for 7 days with varying FA contents; (**d**) specimens of 54 wt.% FA, 0.01 wt.% As^V, 10 M NaOH, and cured for different days. (**C**: Ca_2SiO_4; **C₁**: $CaCO_3$; **C₂**: $Ca_5(SiO_4)_2(OH)_2$; **Q**: quartz)

Immobilization mechanism of As^V. To better understand the underlying mechanism responsible for As^V immobilization, several geopolymer specimens were collected and ground into fine powders for microstructural characterization (e.g., XRD, SEM, and FTIR). XRD patterns of geopolymer specimens show evidence for calcium silicate (Ca_2SiO_4, JCPDS #31-0302), calcite ($CaCO_3$, JCPDS #05-0586), calcium silicate hydroxide (CSH, $Ca_5(SiO_4)_2(OH)_2$, JCPDS #29-0380), quartz (SiO_2, JCPDS #46-1045), and amorphous phases (Figures 4, S5−7), all of which were commonly observed in fly ash-based geopolymers.[31-32, 34, 41] Of all specimens containing As^V, no evidence for crystalline calcium arsenate was identified, suggesting that precipitation with calcium

ions seems not to be the major mechanism for As^V immobilization in these geopolymer specimens. This is, however, contrary to preceding studies of stabilizing arsenic wastes at high levels with calcium-rich cementitious materials [9, 12, 20, 38] and is likely due to the low As^V loadings (i.e., 0.01 – 0.05 wt.%) in this study.

Furthermore, it is worthy to note that increasing the As^V contents appears to enhance the phase transition from amorphous to crystalline (Figures 4a and S5), with the highest crystallinity of the specimen containing the maximum As^V content (i.e., 0.05 wt.%). This has also been observed in previous reports[9, 18] and is likely owing to the hydration inhibition of geopolymer gel by arsenate. The NaOH concentration is also observed to have a profound effect on the phase composition of the geopolymer, and Figures 4b and S6 illustrate the relationship between the NaOH concentration and the crystalline phase composition. There is an increase in the intensity of reflections at $2\theta \sim 26.8°$ and 29.3° (attributed to calcium silicate and CSH, respectively) with increasing NaOH concentration, indicating that higher NaOH concentration accelerates the much more and faster formation of both calcium silicate and CSH, which is good agreement with the above discussion. Besides, CSH is believed to act as an effective encapsulator and physical barrier to prevent the leaching of toxic elements from the geopolymer.[23, 48] This might explain why the specimens activated with 10 M NaOH demonstrated the best S/S performance towards As^V (Figure 3 and Table 2). Of these specimens activated with 10 M NaOH, those with 54 wt.% FA and 0.01 wt.% As^V demonstrated a greater amount of amorphous geopolymer gels as compared to other specimens with different FA and As^V contents (Figures 4a, 4c). Since the amorphous gel is likely to form a more compact geopolymer network than the specimens dominated by crystalline phases,[16, 18] and thereby leading to the maximum UCS (Figure 2d) and the best S/S performance. As discussed earlier and expected, prolonging the curing time will eventually improve the development of crystalline phases (Figures 4d, S7), resulting in loss of the compactness, and thus a slight decrease in the 28-day UCS values (Figure 2d and the supplementary UCS data). It is of interest to note, however, that the specimens with 54 wt.% and 10 M NaOH (i.e., the FMA10G-02 series) showed improved S/S performance towards As^V with increasing curing time (Figure 3c–d, Table 2), regardless of the slight reduction in the 28-day UCS values (Figure 2d). This observation reflects that As^V appears to be incorporated into the crystalline minerals (e.g., calcium silicate and CSH) during the phase transition processes as a result of prolonging the curing time.[3, 19]

SEM images of geopolymer specimens with 54 wt.% FA are shown in Figures 5, 6, and S8. Obviously, three distinct particulates, i.e., the partially and unreacted FA particles, the unreacted MT, and the resultant geopolymer gels, can be identified. The unreacted FA particles are attached or surrounded by the gels which also consolidate and embed some partially reacted FA particles (Figures 5, 6, and S8). No kidney bean-shaped particles corresponding to GY can be found even in specimens with a GY content of 5 wt.% (Figure S8), implying high reactivity of GY

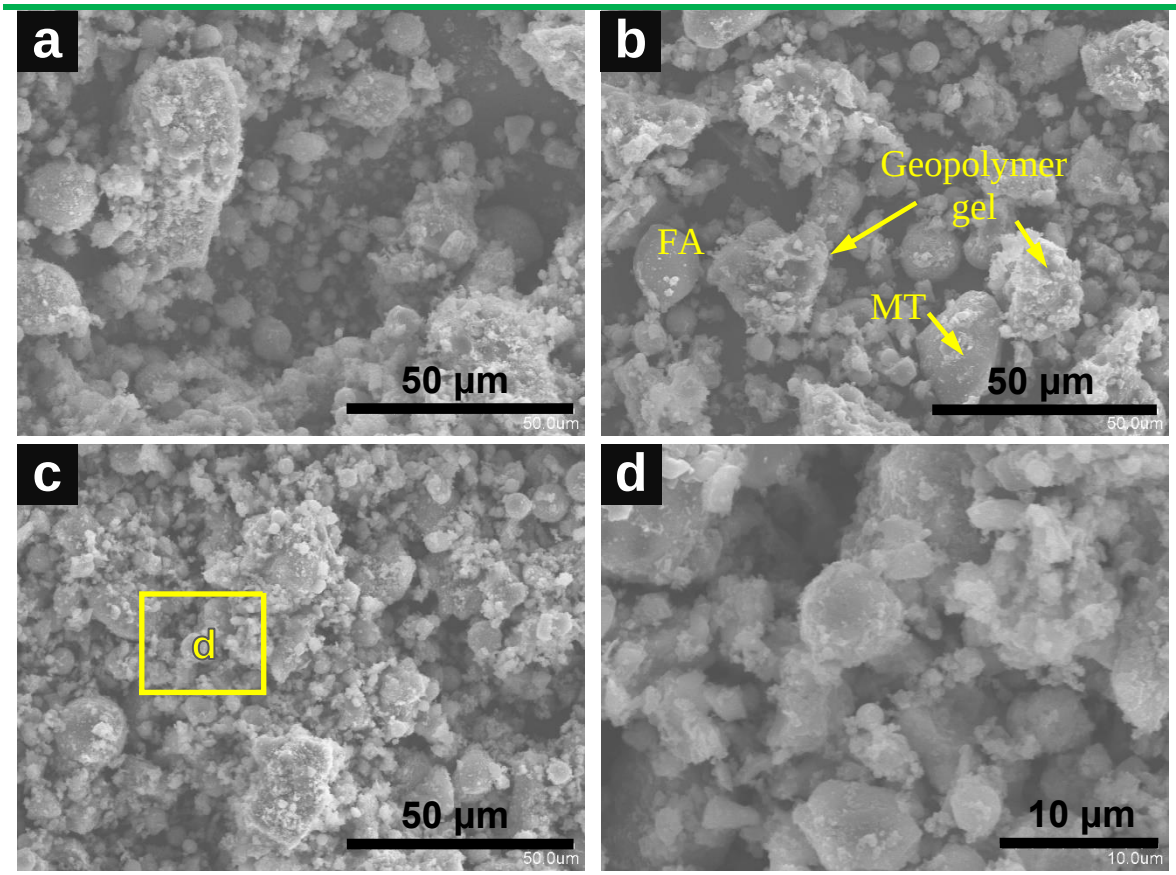

Figure 5 | SEM images of geopolymer specimens of 54 wt.% FA, cured for 7 days and activated with (**a**) 5 M NaOH, (**b**) 8 M NaOH, and (**c**, **d**) 10 M NaOH.

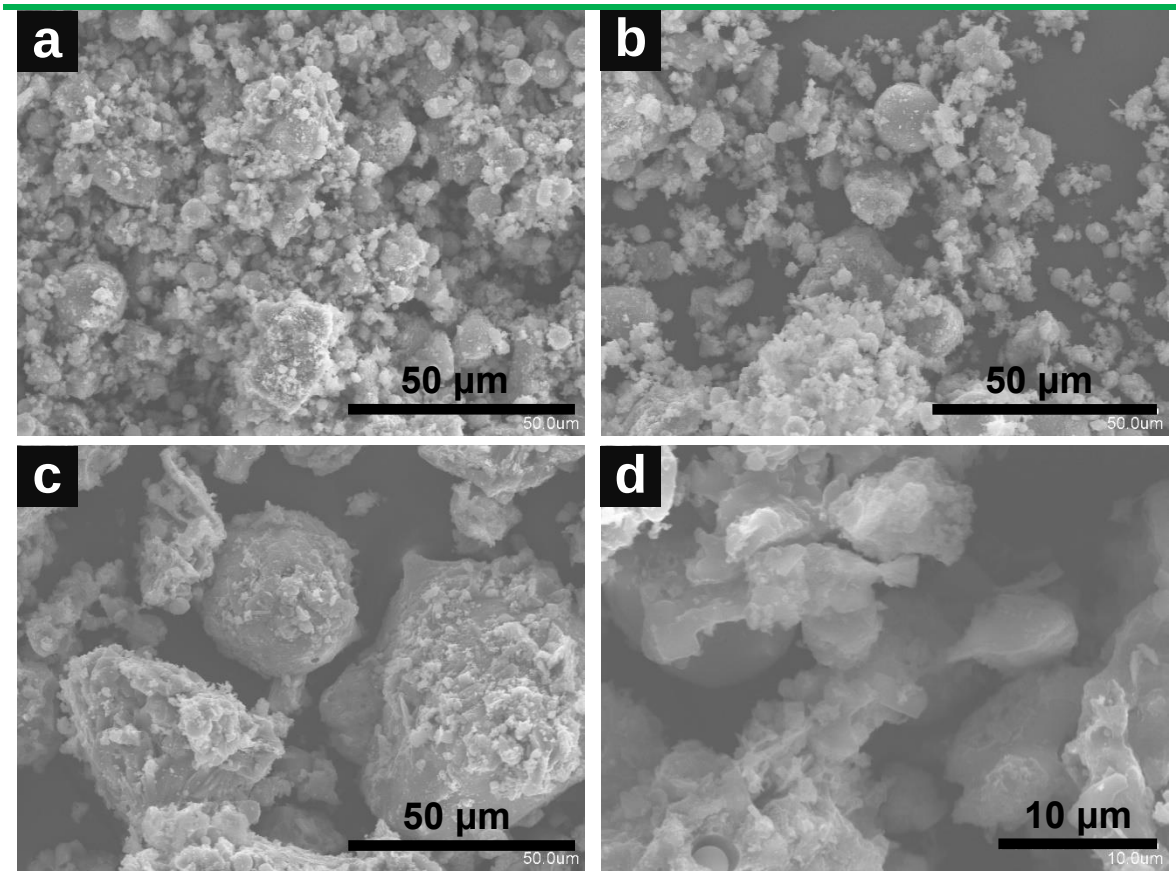

Figure 6 | SEM images of geopolymer specimens of 54 wt.% FA activated with 10 M NaOH and cured for (**a**) 7 days, (**b**) 14 days, and (**c**, **d**) 28 days.

particles in the geopolymerization reaction. Comparison of the micrographs in Figure 5 indicates that as the NaOH concentration increased from 5 to 10 M, the number of unreacted FA particles decreased apparently and the specimens became more compact, implying a higher degree of geopolymerization at higher NaOH concentration,[32, 42] which further confirms the above XRD results in Figure 4. This observation provides direct microscopical evidence of the superior performance of specimens with 54 wt.% FA and 10 M NaOH in both the compressive strength and the As^V immobilization (Figures 2, 3, and Table 2). Moreover, note that there is no significant change in the microstructure of the specimens with 54 wt.% and 10 M NaOH after curing for 7 days (*cf.* Figure 6b & c), confirming the UCS results that a large portion of the UCS was obtained within 7 days (Figure 2d).[42]

The FTIR spectra of geopolymer specimens with 54 wt.% FA are shown in Figure 7. The assignment of characteristic IR bands based on previous studies is summarized in Table 3. Apparently, neither vibrational band attributed to the symmetric stretching of As-O bond for the adsorbed As^V (i.e., ~ 830 cm^{-1}), nor bands associated with calcium arsenate (i.e., ~ 860 cm^{-1}) are identifiable in both IR spectra, suggesting that neither adsorption nor co-precipitation with calcium ions is likely to contribute to As^V immobilization.[12] This is in good consistency with the above XRD results (Figure 4). In general, the major Si-O-Si vibration band of the raw FA will undergo broadening and shifting toward a lower the curing time.[3, 19] wavenumber after geopolymerization owing to the transition of ordered Si-O-Si structure to a less ordered structure with randomly distributed Si-O-Al bonds.[32, 49] Comparison of the geopolymer IR spectra with that of FA reflects a clear shift of band at 1069 cm^{-1} (assignable to Si-O-Si/Al vibration) to a lower wavenumber at 1002 cm^{-1}, confirming the formation of geopolymer gels with a less ordered network as evidenced by the XRD data (Figure 4). Besides, the intensity of the Si-O-Si/Al vibration bands near 1000 cm^{-1} decreased clearly with increasing As^V contents, indicating the reduction of the geopolymer gel amount as the As^V content increased. This is in good agreement with the above XRD results in Figure 4a. It is worthy to note that the bands of asymmetric stretching vibration (v_3, $-CO_3$) in surface $CaCO_3$ at 1438 and 1485 cm^{-1} weaken as well with increasing As^V contents (Figure 7a). This observation can be explained by the fact that the specimen with the least As^V content (i.e., FMA10G-02a) holds the maximum amorphous phases (Figure 4a), which are more reactive than the crystalline phases in specimens with higher As^V content (i.e., FMA10G-02b, and FMA10G-02c, see Figure 4a) to react with CO_2 in the air to form the surface $CaCO_3$. Given the above results, As^V is likely to be immobilized in the geopolymer gels by physical encapsulation after curing for a short period (e.g., 2 – 7 days),[20, 22-23] and then to be incorporated into the crystalline minerals (e.g., calcium silicate and CSH) during the phase transition processes as a result of prolonging the curing time.[3, 19]

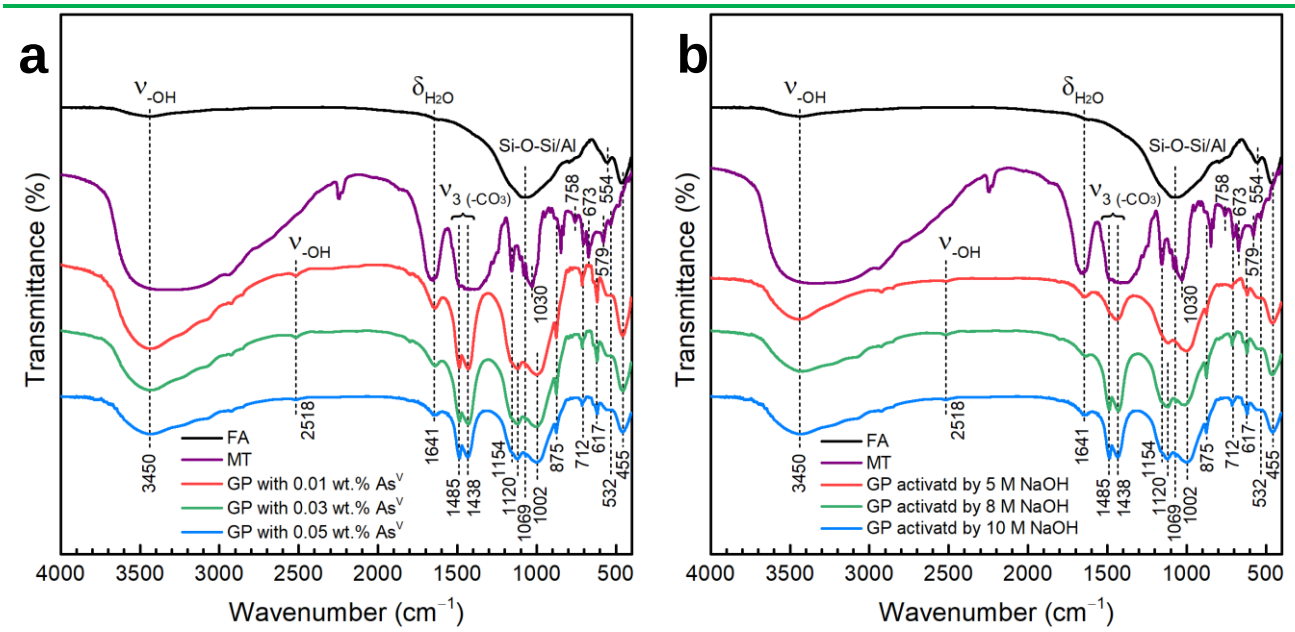

Figure 7 | FTIR spectra of the geopolymer specimens with 54 wt.% FA curried for 7 days: (a) activated with 10 M NaOH and blended with varying As^V contents, (b) blended with 0.05 wt.% As^V and activated with different concentrations of NaOH. The spectra of both the FA and the MT are also presented for comparison.

Table 3 | Assignment of characteristic vibrations to individual band in the geopolymer FTIR spectra.

Wavenumber (cm^{-1})	Characteristic vibrations	Reference
3550–3225, 3450	stretching (−OH)	25, 32, 50
1798	$v_1 + v_4$ ($-CO_3$)	51
1641	bending (H−O−H)	3, 50
1485	asymmetric stretching (v_3, $-CO_3$)	40, 51
1438	asymmetric stretching (v_3, $-CO_3$)	3, 23, 51
950-1200	stretching (Si-O-Si, Si-O-Al)	31-32, 50, 52
1154	asymmetric stretching (Si−O−Si)	23, 31
1120	asymmetric stretching (Si−O−Si, Si−O−Al)	52
1069	asymmetric stretching (Si−O−Si, Si−O−Al), symmetric stretching (v_1, $-CO_3$)	23, 51-52
1030	asymmetric stretching (Si−O−Si, Si−O−Al), symmetric stretching (v_1, $-CO_3$)	31, 40, 51
1002	symmetric stretching (v_1, $-CO_3$), Si−O in Q^2 sites	40, 51
875	out-of-plane bending (v_2, $-CO_3$)	12, 32, 51
758	bending (Si−O−Si, Si−O−Al)	23, 40
712	in-plane bending (v_4, $-CO_3$)	3, 12, 51
673	bending (Si−O−Si, in CSH)	39, 50
617	stretching (Si−O−Si, Si−O−Al)	52
579	bending (Si−O−Si, Si−O−Al)	23
554	bending (Si−O−Al)	23, 52
532	internal deformation of SiO_4	23, 50
455	bending (Si−O−Si)	50

CONCLUSION

Using fly ash, lead-zinc mine tailing, and FGD gypsum as the parent materials, a mixture of sodium hydroxide and sodium silicate solution as the alkali activator, geopolymer specimens were prepared and evaluated for their performance in both the compressive strength and the solidification/stabilization of arsenate from solid wastes in the current study. During the geopolymerization process, the increase in NaOH concentration accelerated the dissolution of aluminosilicate phases and thereby the formation of geopolymer, with increased alkalinity increasing the mechanical strength of the resultant geopolymer specimens. The compressive strength of geopolymer specimens increased with increasing fly ash content to a maximum of 54 wt.%, beyond which the strength was reduced probably due to exceeding the optimum Na/Al ratio at a very high fly ash content. The presence of arsenate appears to enhance the development of geopolymer strength when its content is at most 0.03 wt.%, beyond which the

strength was declined slightly owing to the same reason as mentioned above. However, all the specimens demonstrated excellent performance in the TCLP leaching tests for both arsenate and other heavy metal ions, with all complying with the Chinese leaching standard. Microstructural analyses suggest that arsenate is likely to be physically encapsulated along with the formation of geopolymer gels at first, and this physical-fixed As^{V} may then be incorporated into the crystalline minerals (e.g., calcium silicate and CSH) during phase transition processes. The fly ash/mine tailing-based geopolymers presented here can be potentially used as low-carbon S/S materials for arsenic-contaminated soil remediation and as building materials given their superior mechanical strengths.

ASSOCIATED CONTENT

The Supporting Information is available free of charge on the ACS Publications website.

AUTHOR INFORMATION

Corresponding Author

Feihu Li − Collaborative Innovation Centre of Atmospheric Environment and Equipment Technology, Jiangsu Key Laboratory of Atmospheric Environment Monitoring and Pollution Control, School of Environmental Science and Engineering, Nanjing University of Information Science and Technology (NUIST), 219 Ningliu Road, Nanjing 210044, China; orcid.org/0000-0002-2969-8276; Email: fhli@nuist.edu.cn

Authors

Alseny Bah − Collaborative Innovation Centre of Atmospheric Environment and Equipment Technology, Jiangsu Key Laboratory of Atmospheric Environment Monitoring and Pollution Control, School of Environmental Science and Engineering, Nanjing University of Information Science and Technology (NUIST), 219 Ningliu Road, Nanjing 210044, China

Jie Jin − Collaborative Innovation Centre of Atmospheric Environment and Equipment Technology, Jiangsu Key Laboratory of Atmospheric Environment Monitoring and Pollution Control, School of Environmental Science and Engineering, Nanjing University of Information Science and Technology (NUIST), 219 Ningliu Road, Nanjing 210044, China

Andrea O. Ramos − Collaborative Innovation Centre of Atmospheric Environment and Equipment Technology, Jiangsu Key Laboratory of Atmospheric Environment Monitoring and Pollution Control, School of Environmental Science and Engineering, Nanjing University of Information Science and Technology (NUIST), 219 Ningliu Road, Nanjing 210044, China

Author Contributions

F.L. designed and supervised the research; A.B., J.J., and A. R. performed the research; all authors analyzed the data; and F.L. and J.J. wrote the paper with inputs from all other authors.

Notes

The authors declare no competing financial interest.

ACKNOWLEDGMENTS

The work was partially supported by the National Natural Science Foundation of China (51002080, 51310105009).

REFERENCES

1. Podgorski, J.; Berg, M., Global threat of arsenic in groundwater. *Science* **2020,** *368* (6493), 845-850.
2. Li, Y. C.; Min, X. B.; Chai, L. Y.; Shi, M. Q.; Tang, C. J.; Wang, Q. W.; Liang, Y. J.; Lei, J.; Liyang, W. J., Co-treatment of gypsum sludge and Pb/Zn smelting slag for the solidification of sludge containing arsenic and heavy metals. *J. Environ. Manage.* **2016,** *181*, 756-761.
3. Li, Y. C.; Min, X. B.; Ke, Y.; Fei, J. C.; Liu, D. G.; Tang, C. J., Immobilization potential and immobilization mechanism of arsenic in cemented paste backfill. *Miner. Eng.* **2019,** *138*, 101-107.
4. Singh, R.; Singh, S.; Parihar, P.; Singh, V. P.; Prasad, S. M., Arsenic contamination, consequences and remediation techniques: A review. *Ecotoxicol. Environ. Saf.* **2015,** *112*, 247-270.
5. Nidheesh, P. V.; Singh, T. S. A., Arsenic removal by electrocoagulation process: Recent trends and removal mechanism. *Chemosphere* **2017,** *181*, 418-432.
6. Wang, C.; Luan, J.; Wu, C., Metal-organic frameworks for aquatic arsenic removal. *Water Res.* **2019,** *158*, 370-382.
7. Liu, B.; Kim, K. H.; Kumar, V.; Kim, S., A review of functional sorbents for adsorptive removal of arsenic ions in aqueous systems. *J. Hazard. Mater.* **2020,** *388*, 121815.
8. Alka, S.; Shahir, S.; Ibrahim, N.; Ndejiko, M. J.; Vo, D. V. N.; Abd Manan, F., Arsenic removal technologies and future trends: A mini review. *J. Clean. Prod.* **2021,** *278*, 123805.
9. Wang, L.; Cho, D. W.; Tsang, D. C. W.; Cao, X. D.; Hou, D. Y.; Shen, Z. T.; Alessi, D. S.; Ok, Y. S.; Poon, C. S., Green remediation of As and Pb contaminated soil using cement-free clay-based stabilization/solidification. *Environ. Int.* **2019,** *126*, 336-345.
10. Palansooriya, K. N.; Shaheen, S. M.; Chen, S. S.; Tsang, D. C. W.; Hashimoto, Y.; Hou, D. Y.; Bolan, N. S.; Rinklebe, J.; Ok, Y. S., Soil amendments for immobilization of potentially toxic elements in contaminated soils: A critical review. *Environ. Int.* **2020,** *134*, 105046.
11. Dutre, V.; Vandecasteele, C., Immobilization mechanism of arsenic in waste solidified using cement and lime. *Environ. Sci. Technol.* **1998,** *32* (18), 2782-2787.
12. Jing, C. Y.; Korfiatis, G. P.; Meng, X. G., Immobilization mechanisms of arsenate in iron hydroxide sludge stabilized with cement. *Environ. Sci. Technol.* **2003,** *37* (21), 5050-5056.
13. Singh, T. S.; Pant, K. K., Solidification/stabilization of arsenic containing solid wastes using portland cement, fly ash and polymeric materials. *J. Hazard. Mater.* **2006,** *131* (1-3), 29-36.
14. Choi, W. H.; Lee, S. R.; Park, J. Y., Cement based solidification/stabilization of arsenic-contaminated mine tailings. *Waste Manage.* **2009,** *29* (5), 1766-1771.
15. Wang, L.; Chen, L.; Guo, B. L.; Tsang, D. C. W.; Huang, L. B.; Ok, Y. S.; Mechtcherine, V., Red mud-enhanced magnesium phosphate cement for remediation of Pb and As contaminated soil. *J. Hazard. Mater.* **2020,** *400*, 123317.
16. Devi, P.; Kothari, P.; Dalai, A. K., Stabilization and solidification of arsenic and iron contaminated canola meal biochar using chemically modified phosphate binders. *J. Hazard. Mater.* **2020,** *385*, 121559.
17. Shi, C. J.; Qu, B.; Provis, J. L., Recent progress in low-carbon binders. *Cem. Concr. Res.* **2019,** *122*, 227-250.
18. Tian, Q. Z.; Chen, C. S.; Wang, M. M.; Guo, B. L.; Zhang, H. J.; Sasaki, K., Effect of Si/Al molar ratio on the immobilization of selenium and arsenic oxyanions in geopolymer. *Environ. Pollut.* **2021,** *274*, 116509.
19. Zhou, X.; Zhang, Z. F.; Yang, H.; Bao, C. J.; Wang, J. S.; Sun, Y. H.; Liu, D. W.; Shen, P. L.; Su, C., Red mud-metakaolin based cementitious material for remediation of arsenic pollution: Stabilization mechanism and leaching behavior of arsenic in lollingite. *J. Environ. Manage.* **2021,** *300*, 113715.

20. Jiang, G. H.; Min, X. B.; Ke, Y.; Liang, Y. J.; Yan, X.; Xu, W. B.; Lin, Z., Solidification/stabilization of highly toxic arsenic-alkali residue by MSWI fly ash-based cementitious material containing Friedel's salt: Efficiency and mechanism. *J. Hazard. Mater.* **2022,** *425*, 127992.
21. Diaz-Loya, E. I.; Allouche, E. N.; Eklund, S.; Joshi, A. R.; Kupwade-Patil, K., Toxicity mitigation and solidification of municipal solid waste incinerator fly ash using alkaline activated coal ash. *Waste Manage.* **2012,** *32* (8), 1521-1527.
22. Liu, D. G.; Ke, Y.; Min, X. B.; Liang, Y. J.; Wang, Z. B.; Li, Y. C.; Fei, J. C.; Yao, L. W.; Xu, H.; Jiang, G. H., Cotreatment of MSWI Fly Ash and Granulated Lead Smelting Slag Using a Geopolymer System. *Int. J. Environ. Res. Public Health* **2019,** *16* (1), 156.
23. Opiso, E. M.; Tabelin, C. B.; Maestre, C. V.; Aseniero, J. P. J.; Park, I.; Villacorte-Tabelin, M., Synthesis and characterization of coal fly ash and palm oil fuel ash modified artisanal and small-scale gold mine (ASGM) tailings based geopolymer using sugar mill lime sludge as Ca-based activator. *Heliyon* **2021,** *7* (4), e06654.
24. Kavitha, O. R.; Shanthi, V. M.; Arulraj, G. P.; Sivakumar, V. R., Microstructural studies on eco-friendly and durable Self-compacting concrete blended with metakaolin. *Appl. Clay Sci.* **2016,** *124*, 143-149.
25. Ahmari, S.; Zhang, L. Y., Production of eco-friendly bricks from copper mine tailings through geopolymerization. *Constr. Build. Mater.* **2012,** *29*, 323-331.
26. Moukannaa, S.; Nazari, A.; Bagheri, A.; Loutou, M.; Sanjayan, J. G.; Hakkou, R., Alkaline fused phosphate mine tailings for geopolymer mortar synthesis: Thermal stability, mechanical and microstructural properties. *J. Non-Cryst. Solids* **2019,** *511*, 76-85.
27. Bah, A.; Feng, D. L.; Kedjanyi, E. A. K.; Shen, Z. Y.; Bah, A.; Li, F. H., Solidification of (Pb–Zn) mine tailings by fly ash-based geopolymer I: influence of alkali reagents ratio and curing condition on compressive strength. *J. Mater. Cycles Waste Manage.* **2022,** *24* (1), 351-363.
28. Izquierdo, M.; Querol, X.; Davidovits, J.; Antenucci, D.; Nugteren, H.; Fernandez-Pereira, C., Coal fly ash-slag-based geopolymers: Microstructure and metal leaching. *J. Hazard. Mater.* **2009,** *166* (1), 561-566.
29. Giels, M.; Iacobescu, R. I.; Cappuyns, V.; Pontikes, Y.; Elsen, J., Understanding the leaching behavior of inorganic polymers made of iron rich slags. *J. Clean. Prod.* **2019,** *238*, 117736.
30. U.S. Environmental Protection Agency, Method 1311: Toxicity Characteristic Leaching Procedure. Washington, DC, 1992.
31. Rees, C. A.; Provis, J. L.; Lukey, G. C.; van Deventer, J. S. J., In situ ATR-FTIR study of the early stages of fly ash geopolymer gel formation. *Langmuir* **2007,** *23* (17), 9076-9082.
32. Ahmari, S.; Ren, X.; Toufigh, V.; Zhang, L. Y., Production of geopolymeric binder from blended waste concrete powder and fly ash. *Constr. Build. Mater.* **2012,** *35*, 718-729.
33. van Jaarsveld, J. G. S.; van Deventer, J. S. J., Effect of the alkali metal activator on the properties of fly ash-based geopolymers. *Ind. Eng. Chem. Res.* **1999,** *38* (10), 3932-3941.
34. Li, Q.; Xu, H.; Li, F. H.; Li, P. M.; Shen, L. F.; Zhai, J. P., Synthesis of geopolymer composites from blends of CFBC fly and bottom ashes. *Fuel* **2012,** *97*, 366-372.
35. Allahverdi, A.; Kani, E. N., Construction Wastes as Raw Materials for Geopolymer Binders. *Int. J. Civ. Eng.* **2009,** *7* (3), 154-160.
36. Rowles, M.; O'Connor, B., Chemical optimisation of the compressive strength of aluminosilicate geopolymers synthesised by sodium silicate activation of metakaolinite. *J. Mater. Chem.* **2003,** *13* (5), 1161-1165.
37. Shan, C. C.; Jing, Z. Z.; Pu, L.; Pan, X. H., Solidification of MSWI Ash at Low Temperature of 100 degrees C. *Ind. Eng. Chem. Res.* **2012,** *51* (28), 9540-9545.
38. Zhang, D. N.; Yuan, Z. D.; Wang, S. F.; Jia, Y. F.; Demopoulos, G. P., Incorporation of arsenic into gypsum: Relevant to arsenic removal and immobilization process in hydrometallurgical industry. *J. Hazard. Mater.* **2015,** *300*, 272-280.
39. Zhang, Y. Y.; Zhang, S. Q.; Ni, W.; Yan, Q. H.; Gao, W.; Li, Y. Y., Immobilisation of high-arsenic-containing tailings by using metallurgical slag-cementing materials. *Chemosphere* **2019,** *223*, 117-123.
40. Tigue, A. A. S.; Malenab, R. A. J.; Dungca, J. R.; Yu, D. E. C.; Promentilla, M. A. B., Chemical Stability and Leaching Behavior of One-Part Geopolymer from Soil and Coal Fly Ash Mixtures. *Minerals* **2018,** *8* (9), 411.
41. van Jaarsveld, J. G. S.; van Deventer, J. S. J.; Lukey, G. C., The effect of composition and temperature on the properties of fly ash- and kaolinite-based geopolymers. *Chem. Eng. J.* **2002,** *89* (1-3), 63-73.
42. Zhang, L. Y.; Ahmari, S.; Zhang, J. H., Synthesis and characterization of fly ash modified mine tailings-based geopolymers. *Constr. Build. Mater.* **2011,** *25* (9), 3773-3781.
43. Shadnia, R.; Zhang, L. Y., Experimental Study of Geopolymer Synthesized with Class F Fly Ash and Low-Calcium Slag. *J. Mater. Civ. Eng.* **2017,** *29* (10), 04017195.
44. Rovnanik, P., Effect of curing temperature on the development of hard structure of metakaolin-based geopolymer. *Constr. Build. Mater.* **2010,** *24* (7), 1176-1183.
45. Akhter, H.; Cartledge, F. K.; Roy, A.; Tittlebaum, M. E., Solidification/stabilization of arsenic salts: Effects of long cure times. *J. Hazard. Mater.* **1997,** *52* (2-3), 247-264.
46. Clancy, T. M.; Snyder, K. V.; Reddy, R.; Lanzirotti, A.; Amrose, S. E.; Raskin, L.; Hayes, K. F., Evaluating the cement stabilization of arsenic-bearing iron wastes from drinking water treatment. *J. Hazard. Mater.* **2015,** *300*, 522-529.
47. PRC Ministry of Ecology and Environment, Identification Standards for Hazardous Wastes (GB 5085.3 - 2007). Beijing, China, 2007.
48. Bankowski, P.; Zou, L.; Hodges, R., Using inorganic polymer to reduce leach rates of metals from brown coal fly ash. *Miner. Eng.* **2004,** *17* (2), 159-166.
49. Zhang, W.; Yao, X.; Yang, T.; Liu, C.; Zhang, Z. H., Increasing mechanical strength and acid resistance of geopolymers by incorporating different siliceous materials. *Constr. Build. Mater.* **2018,** *175*, 411-421.
50. Yu, P.; Kirkpatrick, R. J.; Poe, B.; McMillan, P. F.; Cong, X. D., Structure of calcium silicate hydrate (C-S-H): Near-, mid-, and far-infrared spectroscopy. *J. Am. Ceram. Soc.* **1999,** *82* (3), 742-748.
51. Sow, P. Y. IR-Spectroscopic Investigations of the Kinetics of Calcium Carbonate Precipitation. University of Konstanz, Konstanz, Germany, 2016.
52. Lee, W. K. W.; van Deventer, J. S. J., Use of infrared spectroscopy to study geopolymerization of heterogeneous amorphous aluminosificates. *Langmuir* **2003,** *19* (21), 8726-8734.